ISSN 2348-375X

Unique Journal of Engineering and Advanced Sciences

Available online: www.ujconline.net

Research Article

A NOVEL APPROACH TO DIAGNOSE GLAUCOMA BASED ON HYBRID FEATURES IN RETINAL IMAGES

Rathanasabhapathy G*, Jayachandran T, Manikandaprabu N, Brindha S

Assistant Professor, Nandha Engineering College, Erode, Tamil nadu, India

Received: 24-10-2015; Revised: 22-11-2015; Accepted: 20-12-2015

*Corresponding Author: **Rathanasabhapathy G**
Assistant Professor, Nandha Engineering College, Erode, Tamil nadu, India

ABSTRACT

Glaucoma is one of the most common causes of blindness. The number of people having severe vision loss in developing countries. Robust mass screening may help to extend the symptom-free life for affected patients. To realize mass screening requires a cost-effective glaucoma detection method which integrates well with digital medical image processing. To address these requirements, the proposed novel low cost automated glaucoma diagnosis system based on hybrid feature extraction from digital fundus images. This paper discusses a system for the automated identification of normal and glaucoma classes using Higher Order Spectra (HOS), Trace Transform (TT), and Discrete Wavelet Transform (DWT) features. This proposed extracted feature are fed to an Expectation Maximization (EM) classifier which produce 98.91% accuracy, 98% sensitivity and 100%specificity.This was able to identify glaucoma and normal images. Furthermore, we propose a novel integrated index called Glaucoma Risk Index (GRI) which is composed from HOS, TT, and DWT features, to diagnose the unknown class using a single feature. Hence this GRI will aid clinicians to make a faster glaucoma diagnosis during the mass screening of normal/glaucoma images.

Keywords: Glaucoma; retina imaging, computer aided diagnosis, higher order spectra, Trace transform, texture, wavelet, support vector machine.

INTRODUCTION

The main focus is to attempt to achieve such a small cost reduction by proposing a glaucoma diagnosis system based on hybrid feature extraction from digital fundus images. The cost reduction comes from the fact that digital fundus images are less expensive as compared to HRT and feature extraction is done with inexpensive general purpose computing machines. Furthermore, both processes (image taking and feature ex-traction) occur in the digital domain, therefore the proposed glaucoma diagnosis system can be easily incorporated into existing medical and administrative work. These advantages do not constrain the reliability of the diagnosis support system. To be specific, it is shown that the proposed system is able to differentiate fundus images from glaucoma patients from those of a normal control group with an accuracy of 98%. Furthermore, in the proposed novel integrated index, called the Glaucoma Risk Index (GRI), which is made up of higher order spectra (HOS), trace transform (TT), and discrete wavelet transform (DWT) features, to diagnose the unknown class using a single feature.

LITRATURE SURVEY:

Glaucoma is one of the most common causes of blindness. The disease has a mean prevalence of 2.4% for all ages and 4.7% for those aged 75 and above. It is estimated that more than 4 million Americans suffer from glaucoma, and half of them are unaware that they have the disease. Approximately 120,000 Americans are blind as a result of glaucoma, consequently making it responsible for 9_12% of all cases of blindness in the United States. Much of this suffering is preventable, because preventive medicine and surgical treatment, such as mean trabeculectomy, laser surgery, drainage implants, are available. Unfortunately, glaucoma symptoms are painless and the brain compensates gradual vision im-pairment to a considerable extent. Therefore, early diagnosis is important to stop or slow down disease progression. However, due to the high mean prevalence of glaucoma, a significant reduction of end stage glaucoma and blindness requires mass screening. 3 Glaucoma leads to (1) structural changes of the optic nerve head (ONH) and the nerve fibre layer and (2) simultaneous functional failure of the visual field. The disease is diagnosed based on intraocular pressure (IOP), visual field loss tests, 4, 5 and the manual assessment of the ONH via ophthalmoscopy 3 or stereo fundus

imaging.6 Various algorithms have been used to identify typical features such as abnormality of blood vessels 7 and ONH, 8, 9 location and quantitation of micro aneurisms or druse. [10-26] State-of-the-art glaucoma diagnosis is based on Heidelberg retinal tomography (HRT) images. Swindale et al. and Adler et al. have modeled a smooth two-dimensional (2D) surface that ¯t to the ONH of topography images. Damage in the glaucomatous eye was detected using optic disk measures (cup and disk area, height variation using HRT images). This global shape approach was compared with a sector-based analysis by Iester et al. Zangwill et al. have automatically diagnosed glaucoma using optic disk parameters, additional parapapillary parameters, and the support vector machine (EM) classifier. Most of these shape approaches assume a valid segmentation of the optic disk. However, a small error in these segmentation-based techniques may result in significant changes in the measurements and errors in the diagnosis. Furthermore, HRT imaging is an expensive measurement, because both manpower and equipment cost are high. Currently, state-of-the-art glaucoma detection requires mass screening. Hence, the number of measurements is potentially very high and a small cost reduction per measurement will make a large different.

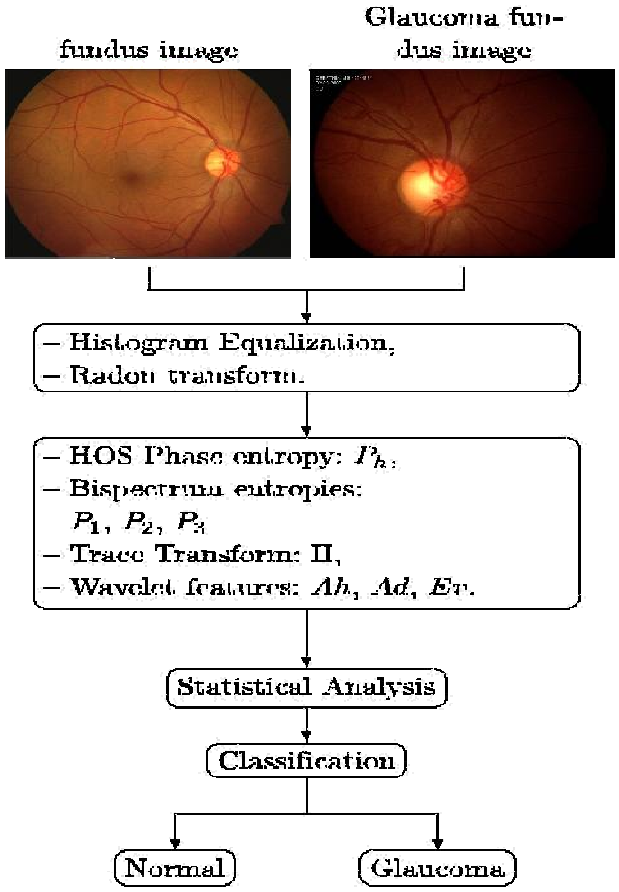

Figure 1: describes the entire flow of our paper

The ethics committee, consisting of senior doctors, approved the images for this research. All images were taken with a resolution of 560 720 pixels and stored in the uncompressed bitmap format. Figure 2 shows representative normal and glaucoma sample images to highlight texture variations between the two groups.

MATERIALS AND METHODS

The following figure shows a block diagram of the proposed system. During the preprocessing stage, colored images are converted to grayscale images and the image contrast is increased with histogram equalization. The Radon transformation converts 2D images into one-dimensional (1D) signals. After these preprocessing steps, important features, namely, phase entropy, spectrum entropy using HOS, triple feature using TT, and average energy of wavelet coefficients are extracted from the image. The statistical significance of these features is evaluated with the independent sample t-test. To evaluate the discriminative powers of these features in a practical setting, they were fed to an EM classifier for automated diagnosis support.

BLOCK DIAGRAM:

The digital retinal images were collected from the Kasturba Medical College, Manipal, India. We have used 60 fundus images _ 30 normal and 30 open-angle glaucoma images from male and female participants who were between 20 and 70 years old. The doctors in the hospital's Ophthalmology Department certified both.The following Fig 1 describes the entire flow of our paper.

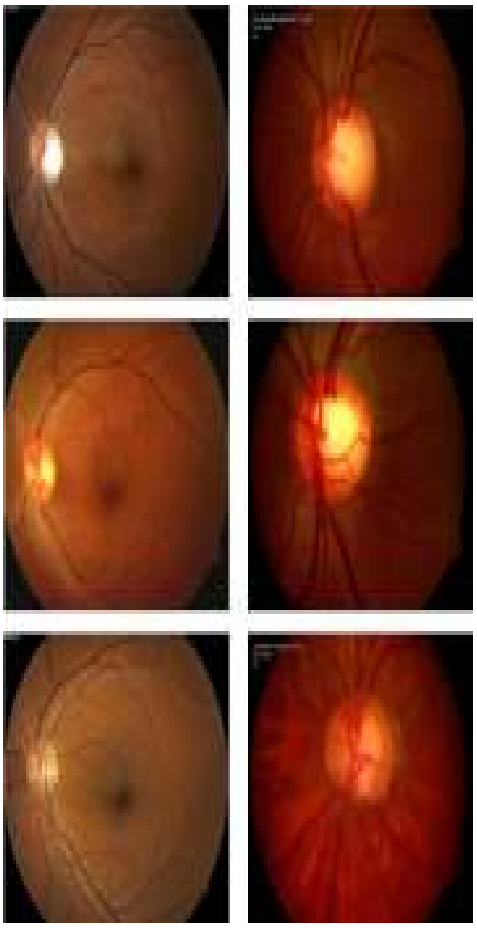

Figure 2: Representative images: Column-(a): Normal; Column-(b): Glaucoma

PREPROCESSING

Preprocessing involves two major steps: (1) histogram equalization and (2) Radon transformation.

HISTOGRAM EQUALIZATION

Enhancing the fundus image contrast will aid the feature extraction process. In this work, colored (RGB) eye images are converted to grayscale images by forming a weighted sum of the R, G, and B components[20-26].

The following fig3 illustrates the Preprocessing stages

Fig. 3. (a) Standard reference image for histogram equalization, (b) grayscale image of (a), (c) histogram of image (b), (d) original glaucoma image, (e) grayscale image of (d), (f) histogram of image (e),(g) histogram equalized image of (e), and (h) histogram of image (g).

RADON TRANSFORM

The Radon transform is widely used in computed tomography to create an image from scattering data which is associated with cross-sectional scans of an object. It transforms 2D images with lines into a domain of possible line parameters, where each line in the image will give a peak that is positioned to reject the corresponding line parameters. Hence, lines in the original image are transformed into points in the Radon domain. The glaucoma image (Fig. 3(g)) is subjected to Radon *transform* with angles varying from 0_180 (with 5 interval). Figure 4 shows the results of the Radon transform for 30 , 90 , and 150.

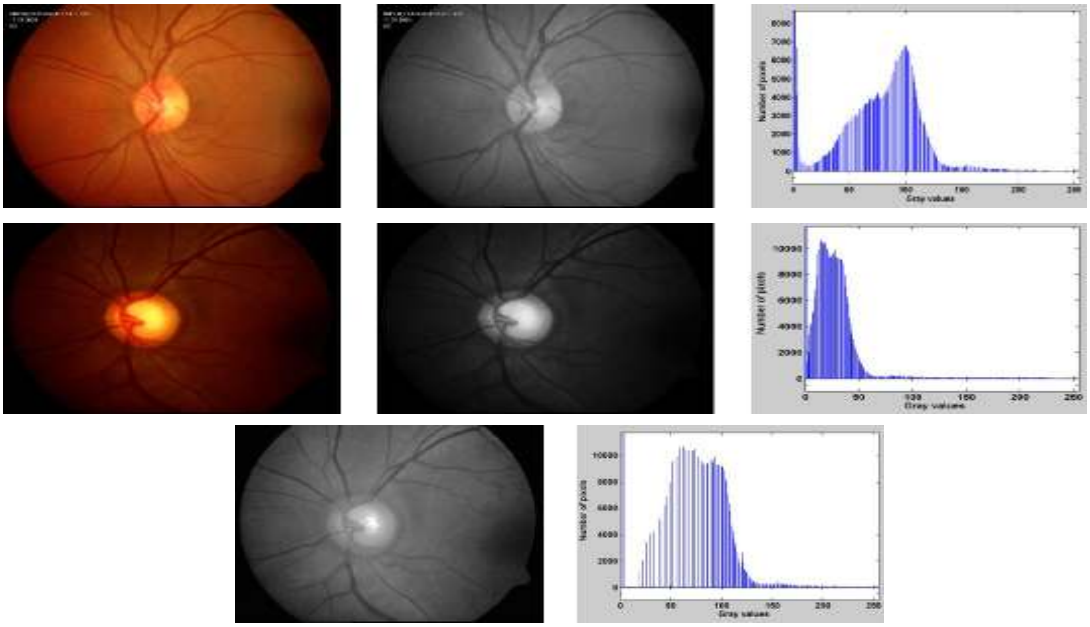

HIGHER ORDER SPECTRA-BASED FEATURES

HOS techniques were ¯rest applied to signal processing problems in 1970.

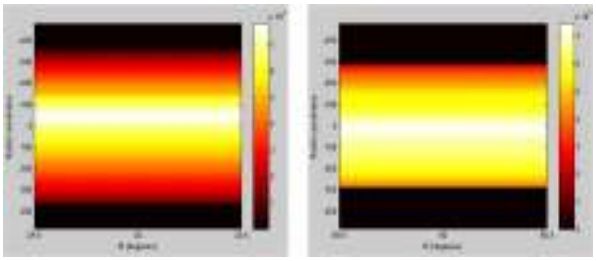

Figure 4 (a): Radon transform image with angle 30 Figure 4 (b): Radon transform image with angle 90

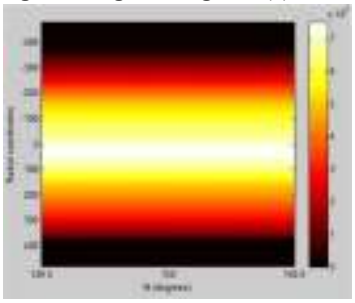

Figure 4 (c): Radon transform image with angle 150

Recent studies show that HOS can be used to diagnose epilepsy using electroencephalogrphy (EEG) signals and cardiac abnormalities using heart rate signals. 27, 28 HOS invariants have been used for shape recognition 29 and to identify different kinds of eye diseases. 4, 20 HOS is a nonlinear method which captures subtle changes in image pixels. The algorithm discussion starts with second order statistics which evaluate both mean value (m) and variance ð.They are denned by expectation operation as follows where \a" is the result of a random process.

TRACE TRANSFORM (TT)

TT is a generalized approach to the Radon transform, and consists of tracing an image with straight lines along certain functional of the so-called image function. The purpose of a functional is to characterize a function by a number. Different functional are used to represent rotation, translation, and scaling invariant features of an image. In many cases, these features correlate well with the visual textures.

The TT can then be denned as a function g based on with the help of T , which is some functional of the image function with variable t. T is called the trace functional. In order to dine a triple feature, two more functional have been denned and they are designated by P and . 19 P is known as the diametrical functional, which is a functional of the TT function when it is considered as a function of the length of the normal to the line only. , called the circus functional, is a functional operating on the orientation variable, after the previous two operations (T and P) have been performed. Thus, the triple feature can be denned as

DISCRETE WAVELET TRANSFORM ENERGY FEATURES

Wavelets are mathematical functions that decompose data into different frequency components and subsequently study each component with a resolution which is matched to its scale. The Fourier transform decomposes a signal into a spectrum of frequencies, whereas the wavelet analysis decomposes a signal into a hierarchy of scales starting from the coarsest scale. 30 This ability to represent an image at various resolutions makes the wavelet transform a better tool for extracting features from images than the Fourier transform.Multiresolution analysis can be done using continuous wavelet transforms (CWT) and DWT. In our work, we have used DWT for feature extraction, which is explained below.

The DWT transform of a 2D signal x is evaluated by sending it through a sequence of down-sampling high and low-pass filters. 33 The low-pass filter isdenned by the transfer function L and the high-pass filter is denned by the transfer function H. The output of the high-pass filter D is known as the detailed coefficients. The following equation shows how these coefficients are obtained:

The low-pass filter output is known as the approximation coefficients. These coefficients are found by using the following equation:

The frequency resolution is further increased by cascading the two basic filter operations. To be specific, the output of the level low-pass filter is fed into the same low- and high-pass filter combination. The detailed coefficients are output at each level and they form the level coefficients. In general, each level halves the number of samples and doubles the frequency resolution. Consequently, in the final level, both detailed and approximation coefficients are obtained as level coefficients.

The level 2D DWT yields four resultant matrices, namely Dh1, Dv1, Dd1, and A1, whose elements are intensity values. The following average and mean value equations were used to extract features from the resultant DWT matrices[11-20].

GLAUCOMA RISK INDEX

We have formulated the GRI based on the significant features listed in Table 1. Our approach follows that of Acharya et al., who have proposed to combine features in such a way that the resulting number or index discriminates normal and disease classes. 24 It is difficult keep track of the individual feature variations. Therefore, we have empirically determined a single integrated index (also called GRI) that is a unique combination of the respective features that results in a unique range for both the classes. The utility of such indices is that they can be more comprehendible to the ophthalmologist than the classifiers which are most times black boxes that directly output the class label. Moreover, it is faster and easier to compute and keep track of these indices. When continuously monitored, the variations in the indices can throw light on how the normal become glaucoma over time. In our case, the GRI dis-criminates fundus images which show glaucoma symptoms from normal fundus images.

EXPECTATION MAXIMIZATION

The EM algorithm iteratively computes expectations (the E step) given a current model, using them as training data to maximize a model estimate (the M step). The reason it works is that the combination of an E and M step is guaranteed to reduce error, and because error is bounded at zero. Therefore, the algorithm must converge. EM works when there is no supervised training data at all. An initial classifier needs to be built randomly (perhaps using a good seeding method like k-means++).Once the first model is initialized, EM deterministically hill climbs until it finds a set of parameters yielding a locally minimum error. Standard operating procedure is to provide a number of different random starting point and choose the best result.

RESULTS

In this study, we have used TT, HOS, and DWT, methods to extract 14 features from digital fundus images. The independent sample t-test was used to establish the statistical significance of these features. All features, with the exception of P1, showed significantly greater values in images taken from glaucomatous participants when compared to the normal control set (Table 1, $p < 0:01$). The low p-values indicate that all features are extremely useful in differentiating normal images from retinal images with glaucomatous appearance. In the case of HOS-based features, spectral entropy based features which, were obtained from Radon transform angles ¼ 0 ; 70 ; 75 ; 80 ; 85 ; 90 , and 180 , were found to be statistically signi¯cant. Among the TT features, 1 was found to statistically signi¯cant. Finally, the DWT features Ad, Av, and Ev, based on bior3.1, were found to be statistically significant. Accuracy (Acc), sensitivity (Sn), specificity (Sp), and positive predictive value (PPV) was calculated for all three trials to obtain the overall performance measures. Table 3 presents the

classification results obtained using significant HOS, TT, and DWT features from the retinal fundus images. The accuracy registered by EM with polynomial and linear kernel was 91.67%.it is presented a summary of the automated glaucoma detection studies which were mentioned in this paper. Many studies have been conducted to develop computer aided decision support systems for the early detection of glaucoma. An artificialneural network (ANN) model, using multifocal visual evoked potential (M-VEP) data, was able to detect glaucoma with a high sensitivity and specificity of 95% and 94%, respectively.

CONCLUSION

In this work, we have presented a new automated glaucoma diagnosis system using a combination of HOS, TT, and DWT features extracted from digital fundus images. Our system, using an EM classifier (with polynomial kernel order 2), was able to detect glaucoma.

REFERENCE

1. Bock R, Meier J, Nyúl LG, Hornegger J, Michelson G, Glaucoma risk index: Automated glaucoma detection from color fundus images, Med Image Anal 2010; 14:471_481.
2. Glaucoma Research Foundation, Glaucoma facts and stats, Retrieved May 1, 2012, from http://www.glaucoma.org/learn/glaucoma facts.php.
3. Nyúl LG, Retinal image analysis for automated glaucoma risk evaluation, in Liu, J, Doi, K, Fenster, A, Chan, SC (eds.), Medical Imaging, Parallel Processing of Images, and Optimization Techniques, SPIE, 2009; 1-9.
4. Acharya UR, Dua S, Du X, VinithaSree S, Chua CK, Automated diagnosis of glaucoma using texture and higher order spectra features, IEEE Trans InfTechnol Biomed, 2011; 15(3): 449-455.
5. Mookiah MRK, Acharya UR, Lim CM, Petznick A, Suri JS, Data mining technique for automated diagnosis of glaucoma using higher order spectra and wavelet energy features, Knowl-Based Syst, 2012; 33(0): 73-82.
6. Lin SC, Singh K, Jampel HD, Hodapp EA, Smith SD, Francis BA, Dueker DK, Fechtner RD, Samples JS, Schuman JS, Minckler DS, Optic nerve head and retinal nerve ¯ber layer analysis: A report by the american academy of ophthalmology, Ophthalmology, 2007; 114(10): 1937_1949.
7. Staal J, Abramo® MD, Niemeijer M, Viergever MA, van Ginneken B, Ridge-based vessel segmentation in color images of the retina, IEEE Trans Med Imaging 23(4):501_509, 2004.
8. Chrastek R, Wolf M, Donath K, Niemann H, Paulus D, Hothorn T, Lausen B, Lämmer R, Mardin CY, Michelson G, Automated segmentation of the optic nerve head for diagnosis of glaucoma, Med Image Anal, 2005; 9(4): 297-314.
9. Hoover A, Goldbaum M, Locating the optic nerve in a retinal image using the fuzzy convergence of the blood vessels, IEEE Trans Med Imaging, 2003; 22(8): 951-958.
10. Walter T, Klein J-C, Automatic detection of microaneurysms in color fundus images of the human retina by means of the bounding box closing, in Proc of the 3rd IntSymp on Med Data Anal, ISMDA '02, Springer-Verlag, London, UK, 2002; 210_220.
11. Jayachandran T and Arulanantham D, Design of Low voltage Comparator for Analog to Digital Conversion, IJAREEIE. 2014; 3: 12.
1. George, Joshni C, Jayachandran T and Marimuthu CN. 2D-DWT Lifting Based Implementation using VLSI architecture." International Journal of Advanced Research in Electronics and Communication Engineering, 2013; 2.3: 363.
2. Kiruthika S, Brindha S. Hiding Protected Scalable Fine-Grained Information Using Access Control." International Journal of Novel Research in Engineering & Pharmaceutical Sciences, 2015; 2.01: 34-38.
12. Abimannan T, Jayachandran T and Marimuthu CN. Content Based Image Retrieval Using Fast 2d Wavelet Transform." International Journal of Innovative Research and Development, 2013; 2.4: 86-96.
13. Jayachandran T, Arulanantham D. Design of Low voltage Comparator for Analog to Digital Conversion. International Journal of Advanced Research in Electrical, Electronics and Instrumentation Engineering, 2014; 3.12: 13697-13703.
14. Lalli, G., Kalamani D and Manikandaprabu N. An ANFIS Based Pattern Recognition Scheme Using Retinal Vascular Tree–A Comparison Approach with Red-Green Channels. Journal of Theoretical and Applied Information Technology 2014; 59.1: 205-212.
15. Manikandaprabu N., Pavithra S and Thilagamani VN. Data Hiding in Color Images. International Journal of Novel Research in Engineering & Pharmaceutical Sciences, 2014; 1: 5.
16. Lalli, G., et al. Feature Recognition on Retinal Fundus Image–A Multi-Systemic Comparative Analysis. International Journal of Advanced Research in Computer Science and Software Engineering, 2013; 3.11: 427-434.
17. Manikandaprabu N., Thilagamani VN and Pavithra S. FPGA Implementation of Image Optimization Algorithms-A Review. International Journal of Novel Research in Engineering & Pharmaceutical Sciences, 2014; 1: 5.
18. Lalli G, Kalamani D and Manikandaprabu N. A New Algorithmic Feature Selection and Ranking for Pattern Recognition on Retinal Vascular Structure with Different Classifiers. Australian Journal of Basic & Applied Sciences, 2014; 8: 15.
19. Roopa VG, Arulpriya KP and Manikandaprabu N. Real Time Visual Tracking of the People using Video

Camera with Reduced Time Complexity. Unique Journal of Engineering and Advanced Sciences, 2014, 2: 1.
20. Jamcey VP and Manikandaprabu N. Hessian Analysis in Multiscale Brain Tumor Segmentation. Unique Journal of Engineering and Advanced Sciences, 2014; 2: 2.
21. Dinsha D and Manikandaprabu N. Breast Tumor Segmentation and Classification using SVM And Bayesian from Thermogram Images." Unique Journal of Engineering and Advanced Sciences, 2014; 2.2: 147-151.
22. Kumar SR et al. Genetic Algorithm based test Pattern Generation for Asynchronous Circuits with Handshake Controllers. Unique Journal of Engineering and Advanced Sciences, 2014; 2: 1.

Source of support: Nil, Conflict of interest: None Declared